Studying protein-reconstituted proteoliposome fusion with content indicators in vitro

Jiajie Diao[1)-6)*], *Minglei Zhao*[1)-5)], *Yunxiang Zhang*[1)-5)], *Minjoung Kyoung*[1)-5)] *and Axel T. Brunger*[1)-5)*]

In vitro reconstitution assays are commonly used to study biological membrane fusion. However, to date, most ensemble and single-vesicle experiments involving SNARE proteins have been performed only with lipid-mixing, but not content-mixing indicators. Through simultaneous detection of lipid and small content-mixing indicators, we found that lipid mixing often occurs seconds prior to content mixing, or without any content mixing at all, during a 50-seconds observation period, for Ca^{2+}-triggered fusion with SNAREs, full-length synaptotagmin-1, and complexin. Our results illustrate the caveats of commonly used bulk lipid-mixing fusion experiments. We recommend that proteoliposome fusion experiments should always employ content-mixing indicators in addition to, or in place of, lipid-mixing indicators.

Keywords:
content mixing; membrane fusion; proteoliposome; single molecule; SNARE

Introduction

Membrane fusion is a process by which two distinct lipid bilayers (membranes) merge their hydrophobic cores to form one interconnected structure. Biological membrane fusion is mediated by the action of integral membrane proteins or membrane-associated proteins. Among fusion proteins, the so-called SNARE proteins play a key role in eukaryotes for vesicle trafficking, secretion, and synchronized neurotransmitter release [1]. Upon Ca^{2+}-triggered synaptic vesicle fusion with the plasma membrane, neurotransmitter molecules are released into the synaptic cleft on a sub-millisecond timescale, transmitting messages across the synaptic cleft between two neurons in the central nervous system or across neuromuscular junctions between a neuron and a muscle.

When complete membrane fusion occurs between two lipid bilayers, a fusion pore is created, allowing exchange of content. Such pore formation is generally preceded by exchange of lipid molecules from both membranes by two-dimensional diffusion. This process, called lipid mixing, is necessary but not sufficient for membrane fusion. For example, hemifusion is a process where the outer leaflets of two membranes merge, but without fusion pore formation.

DOI 10.1002/bies.201300010

[1)] Department of Molecular and Cellular Physiology, Stanford University, Stanford, CA, USA
[2)] Department of Neurology and Neurological Science, Stanford University, Stanford, CA, USA
[3)] Department of Structural Biology, Stanford University, Stanford, CA, USA
[4)] Department of Photon Science, Stanford University, Stanford, CA, USA
[5)] Howard Hughes Medical Institute, Stanford University, Stanford, CA, USA
[6)] Center for Mitochondrial Biology and Medicine, The Key Laboratory of Biomedical Information Engineering of Ministry of Education, School of Life Science and Technology and Frontier Institute of Life Science, Frontier Institute of Science and Technology (FIST), Xi'an Jiaotong University, Xi'an, China

***Corresponding authors:**
Jiajie Diao
E-mail: diaojj@gmail.com
Axel T. Brunger
E-mail: brunger@stanford.edu

Abbreviations:
FRET, Förster resonance energy transfer or fluorescence resonance energy transfer; **SNAREs,** soluble *N*-ethylmaleimide-sensitive factor attachment protein receptors; **TIRF,** total internal reflection fluorescence.

Despite this caveat, lipid-mixing assays have been commonly used to study biological membrane fusion [2] since they are relatively easy to perform and fluorescent lipid labeling of membranes can be readily accomplished.

Historically, the first in vitro lipid-mixing assay with SNARE-reconstituted proteoliposomes used a FRET pair consisting of 7-nitro-2-1,3-benzoxadiazol-4-yl (NBD) and rhodamine [3]. Two sets of vesicles were prepared, one set (referred to as v-vesicles in the following) contained synaptobrevin-2, also referred to as VAMP2 (vesicle associated membrane protein 2), while the other set (referred to as t-vesicles in the following) contained syntaxin-1A and SNAP-25A. V-vesicles were labeled with both NBD and rhodamine such that NBD fluorescence was quenched by rhodamine via Förster resonance energy transfer or fluorescence resonance energy transfer (FRET). When t-vesicles were added to v-vesicles, vesicle hemifusion and/or complete fusion diluted labeled v-vesicle lipids with unlabeled t-vesicle lipids via lipid mixing. As a consequence of the dilution, the average inter-dye distance between NBD and rhodamine increased, and the fluorescence emission intensity from NBD increased. The NBD fluorescence recovery was recorded in bulk solution, representing an ensemble average. This pioneering experiment provided the first evidence that SNARE proteins can mediate membrane hemifusion and/or fusion in vitro.

Although an ensemble lipid-mixing assay is relatively easy to perform, it falls short in revealing information about prefusion (docking) and fusion intermediates, and the time scale for full fusion. Moreover, monitoring lipid mixing alone can be misleading since lipid mixing can occur without or with significantly delayed content mixing, that is the exchange or release of aqueous content: for example, neuronal SNAREs alone did not produce much content mixing, although SNAREs readily induced lipid mixing [4, 5], influenza virus-induced fusion content mixing occurred seconds after initial lipid mixing [6], and content mixing occurred with minute delay after lipid mixing in vacuolar fusion [7]. We recently found an even more striking difference between content mixing and lipid mixing for Ca^{2+}-triggered fusion with SNAREs, full-length synaptotagmin-1, and complexin-1. Through simultaneous observation of both lipid and small content fluorescent dyes, we found that significant lipid mixing can occur seconds before content mixing, or without any content mixing during the observation period of 50 seconds [8].

Content-mixing measurements have been very difficult to achieve with ensemble-based assays since leakiness of proteoliposomes, aggregation, and vesicle rupture lead to false-positive fluorescent signals that are not related to genuine fusion. Another major issue with the commonly used lipid-mixing ensemble experiments is that they cannot assess the relative contribution of docked & unfused and docked & (hemi-)fused vesicles on the overall fusion kinetics [9]. For example, if a factor would enhance docking, it would also enhance subsequent lipid mixing by increasing the number of docked vesicles, rather than affecting the fusion kinetics itself. It is thus necessary to use a single particle optical microscopy method to resolve this ambiguity [10–12]. In addition to our single vesicle system [5, 8, 13] (discussed below), other methods have been developed to distinguish docking from fusion: single-particle fluorescence correlation spectroscopy (FCS) lipid-mixing experiments [9] and single-particle alternating laser excitation lipid-mixing experiments [14].

Boxer and coworkers showed that inner leaflet mixing can occur without complete fusion using an in vitro system where membrane fusion was induced by DNA-zippering [15]. This striking result poses a caveat for assays that rely on inner-leaflet lipid-mixing indicators alone to assess complete fusion (i.e. by chemical reduction of the outer leaflet labels), even when they are performed at the single vesicle level. Moreover, conclusions drawn in the absence of content mixing indicators are often incomplete, or in some cases, they do not correlate well with physiological studies [16]. We therefore recommend that vesicle fusion experiments should always employ a content-mixing indicator in addition to or in place of lipid-mixing indicators.

The single vesicle-vesicle lipid/content mixing assay reveals little correlation between lipid and content mixing

To overcome the shortcomings of both the bulk and single-vesicle lipid mixing assays, we developed a single vesicle-vesicle method that simultaneously monitors both lipid and content mixing using spectrally distinct fluorescent dyes [5, 8, 13]. We reconstituted the synaptic proteins: synaptotagmin-1 & synaptobrevin-2 and syntaxin-1A & SNAP-25A into two separate populations of liposomes, termed v- and t-vesicles, respectively (Fig. 1A). Unlabeled acceptor vesicles were tethered to a glass surface, whereas the donor vesicles were labeled with self-quenched lipid dyes (1,1′-Dioctadecyl-3,3,3′,3′-Tetramethylindodicarbocyanine Perchlorate, DiD) and content dyes (sulforhodamine B). After docking and incubation periods, instances of docked (interacting) v-/t-vesicle pairs were observed by weak fluorescence spots. Upon Ca^{2+} injection, characteristic stepwise increases in the fluorescence intensity from two dyes emerged due to hemifusion or complete fusion events. The stepwise increases in fluorescence intensity can be explained by dilution of the particular dyes upon (hemi-)fusion resulting in partial recovery of the respective fluorescence intensities.

Most recently, we have developed a variant of the incubation protocol of our single vesicle-vesicle assay [8]: v-vesicles were incubated at a low concentration for a longer period, followed by Ca^{2+}-injection (Fig. 1B, left column). Previously we incubated v-vesicles for a short period of time at high concentration, followed by buffer exchange, and subsequent longer incubation period [5, 13] (Fig. 1B, right column). The new method (Fig. 1B, left column) produces more interactions between surface immobilized t-vesicles and free v-vesicles.

Our single vesicle-vesicle microscopy system allowed us to analyze individual events in real-time by inspection of individual fluorescence time traces. We observed multiple fusion pathways including instances of immediate and delayed instances of content and lipid mixing [8]. As an example, the fluorescence intensity time traces shown in Fig. 2A represent the ''classical'' pathway of membrane fusion involving outer leaflet mixing upon Ca^{2+} injection (vertical blue bar), followed by inner leaflet mixing and fusion (Fig. 2A). The

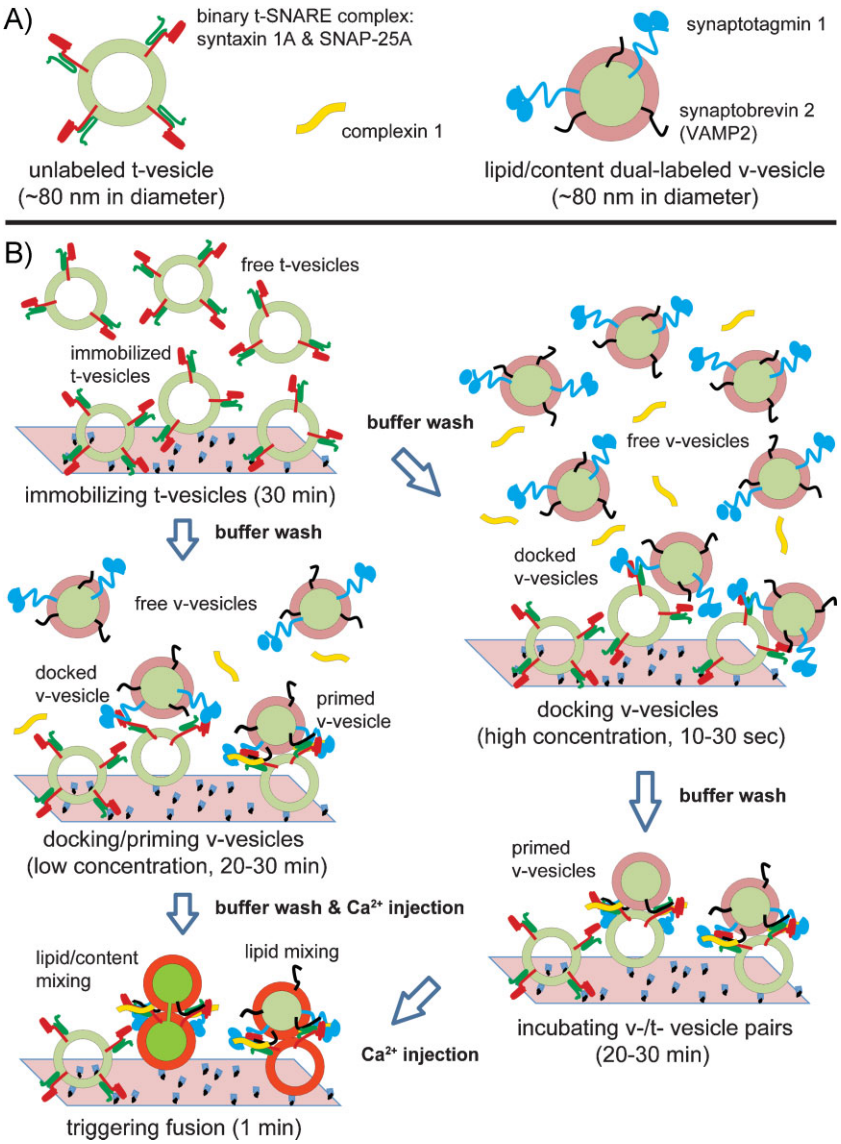

Figure 1. Single vesicle-vesicle fusion assay. **A:** Plasma membrane mimic: unlabeled t-vesicle with syntaxin-1A & SNAP-25A; synaptic vesicle mimic: lipid/content dye dual-labeled v-vesicle reconstituted with synaptobrevin-2 (VAMP2) & synaptotagmin-1, and complexin-1. **B:** Experimental schema. The left panel shows the recently developed protocol: t-vesicles are immobilized, v-vesicles are docked/primed at low concentration, and then Ca^{2+} is injected [8]. Between the steps, buffer exchanges are performed with at least 200 μl vesicle buffer (90 mM NaCl, 20 mM HEPES, 20 μM EGTA, 1% β-mercaptoethanol, pH 7.4). The right panel shows the previous incubation method [5, 13]: v-vesicles are docked at high concentration for a short period, followed by buffer exchange, and then an incubation stage for a longer period. For both methods, Ca^{2+}-triggered fusion events are monitored by observing changes in the fluorescence intensities of the content and lipid dyes, respectively.

second-delay between the two lipid-mixing events suggests a transit through a stable hemifusion membrane intermediate that is most likely a hemifusion diaphragm. For injection at 500 μM Ca^{2+}, both lipid and content mixing events occurred, with approximately >50% of the observed events resulting in only lipid mixing over the observation period of 50 seconds (Fig. 2B). Overall, immediate fusion (a correlate with synchronous neurotransmitter release) was observed in a minority of cases, mimicking the physiological observation that only a subset of synaptic vesicles completely fuse upon Ca^{2+} stimulation in caged Ca^{2+} photolysis experiments [17].

Our single vesicle-vesicle lipid mixing results are consistent with previous studies that utilised only lipid mixing indicators [18–20]. However, the large difference between the observed lipid and content dye fluorescence histograms (Fig. 2B) again calls into question fusion assays that did not utilize content indicators.

Other single vesicle approaches have been used to detect content mixing, such as a single vesicle-vesicle content mixing assay involving surface-immobilized v-vesicles (with reconstituted synaptotagmin-1) encapsulating large Cy3/Cy5 dual-labeled DNA probes and soluble t-vesicles containing complementary DNAs [21, 22]. Once the fusion pore has sufficiently expanded, the two DNA strands hybridize, and thus, induce a conformational change that reduces the observed FRET efficiency. Through single molecule FRET detection of this conformational change, fusion pore expansion, the very late step of membrane fusion process, could be studied [23].

Content mixing indicators have also been introduced in recent ensemble assays to study SNARE-mediated fusion, using Ca^{2+} ions [24] and sulforhodamine B molecules [25]; it should be noted that the use of Ca^{2+} ions as content indicators is problematic due to leakiness of the membranes [26]. In any case, due to the ensemble character of these experiments, fusion intermediates cannot be discerned, and, as mentioned above, effects due to changes in docking or fusion probability cannot not be distinguished.

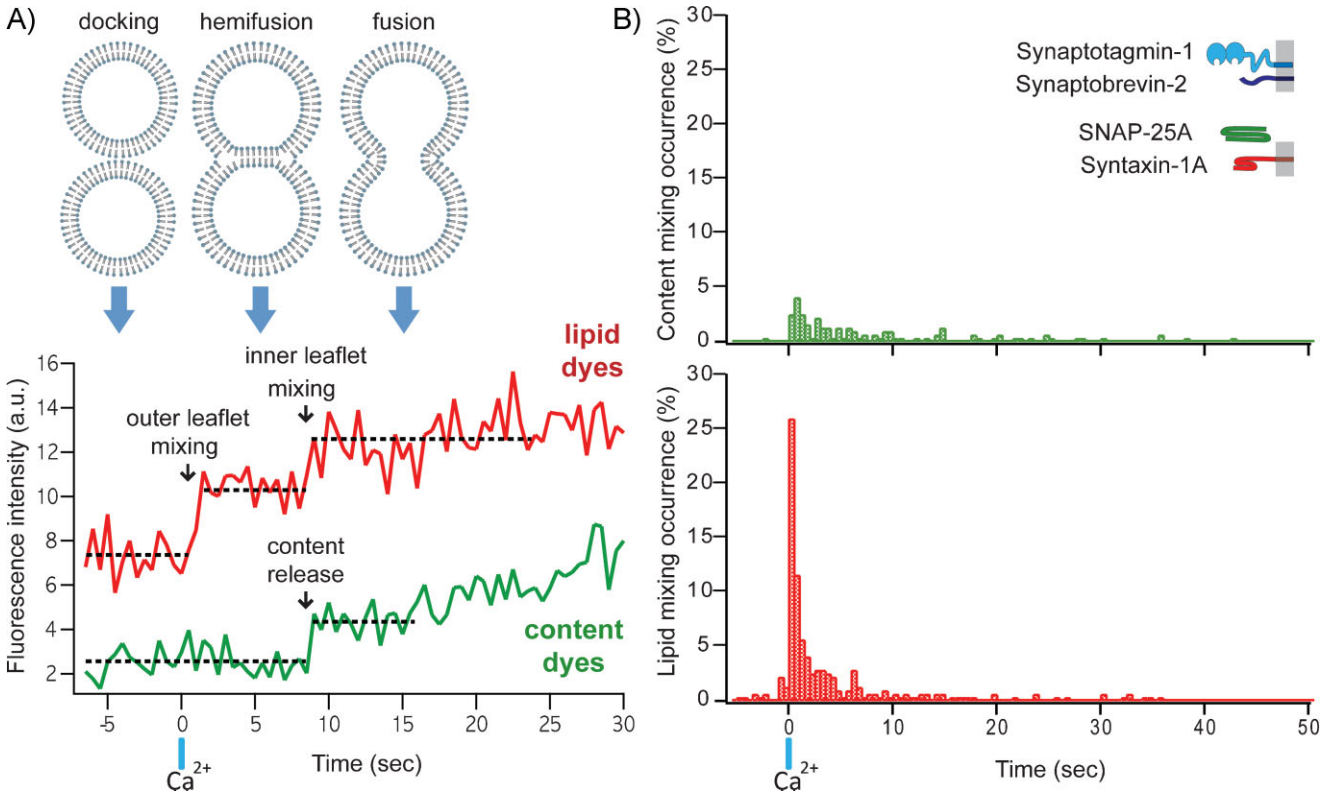

Figure 2. Typical data obtained from the single vesicle-vesicle fusion assay. **A:** Traces of fluorescence intensity against time for a typical lipid dye (red) and a content dye (green). Full fusion is defined as a content mixing fluorescence increase, while hemifusion corresponds to a step increase in lipid fluorescence in the absence of content mixing. Corresponding membrane states are shown above. **B:** Histograms of the occurrence of Ca^{2+}-triggered lipid- (bottom) and content- (top) mixing events for the system consisting of neuronal SNAREs and synaptotagmin-1 using 500 msec time binning for one of multiple experiments (histograms were generated from 321 individual traces). Events during a 7.5-seconds period before Ca^{2+} injection are also shown (if any). Time $t = 0$ corresponds to the instance of 500 μM Ca^{2+}injection as determined by the appearance of cascade-blue fluorescence. Histograms are normalized with respect to the number of total events of lipid mixing.

New software automates data analysis for our single vesicle-vesicle fusion system

Due to the small size of the vesicles (~80 nm in diameter) compared to the detection wavelength of TIRF microscopy, the time-series of fluorescence-emission images was analyzed with similar methods as used for single-molecule TIRF microscopy [5, 27]. Fluorescence-intensity time traces for each individual docked vesicle were generated by integrating pixels within a fixed radius from the centroid of each vesicle (i.e. an observed fluorescent spot) within a selected time bin for both lipid and content dyes. Instances of lipid or content mixing were identified by detection of significant step-increases in the corresponding fluorescence intensity time traces.

Step-increase detection is a common problem in time series analysis. Several techniques have been developed in order to automatically and reliably detect step increase in noisy signal traces, including global methods such as wavelet analysis [28] and total variation de-noising [29]. Other methods use local sliding window methods such as the Student's *t*-test method or nonlinear filtering. To apply these techniques, one should consider the nature of the observed data and the underlying physics of the observed processes. A particular example is the detection of cantilever step increase in atomic force microscopy (AFM) force curves [30].

In our single vesicle-vesicle assay, the fluorescence intensities are relatively stable before and after lipid- or content-mixing events (Fig. 3). The apparent life-time of the dyes used in our assay is in the order of several minutes which is significant longer than the data acquisition time window of about 50 seconds. Hence we used a local sliding window approach by calculating the difference in the average fluorescence intensity level over a fixed size local window before and after a particular time point. We defined a mixing event as a local maximum of these differences as a function of time when the difference exceeded a selected threshold. The threshold was selected as a multiple of the local noise level, σ, before and after the step increase (Fig. 3, red lines). We detected a step-increase by using the following inequality,

$$\frac{\left(\frac{1}{n}\sum_{i=t-n}^{t-1} x_i - \frac{1}{n}\sum_{j=t}^{t+n-1} x_j\right)}{\sqrt{\sigma_-^2 + \sigma_+^2}} \geq \eta_{\text{th}}$$

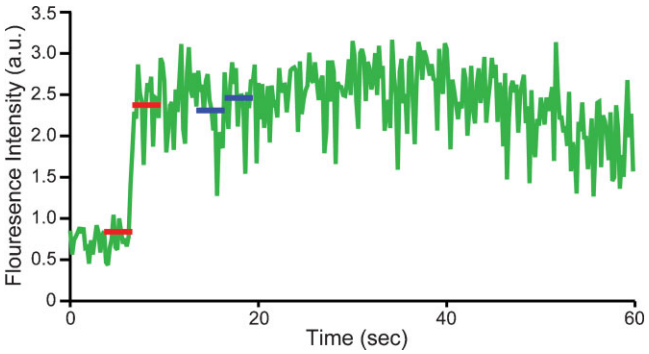

Figure 3. Automated step-increase detection. An example of a content dye fluorescence intensity time trace is shown. Two red lines indicate a step increase greater than a set threshold as determined by the local noise level. The two blue lines represent false-positives that are automatically excluded by the Wald–Wolfowitz test [31].

Here x_i refers to the trace intensity indexed by frame number i and n is the size of local sliding window, σ_- and σ_+ refer to the standard deviation before and after the testing time point, η_{th} is an arbitrary dimensionless threshold to differentiate real jumps from noise fluctuations. We typically used a sliding window size of ~3 seconds and a threshold of 2σ. Due to the smaller number of data points in the sliding window, the Wald–Wolfowitz test [31] can be used to reject false positives caused by monotonicity or periodicity in the local data. The Wald–Wolfowitz test (also known as the ''Runs test'') was used to test the randomness of intensity fluctuations for both the local window before and after selected time points. We rejected time points where the test failed both before and after a particular time point with a given threshold of significance in the Z direction.

Since content mixing is the true indicator of complete membrane fusion, monitoring just content dye fluorescence without a lipid mixing indicator is sufficient to study fusion [32], although in this simpler version of the experiment one is unable to determine the initial state of the membrane before Ca^{2+}-injection (that is, docked vs. hemifused). We automated the detection of content-mixing instances using the definition of step-increase as described in the previous paragraph. Histograms of the observed content mixing instances were then automatically generated in order to obtain information about fusion kinetics. We observed that the majority of the docked vesicles did not proceed to full fusion upon injection of 250–500 μM Ca^{2+} [8], resulting in relatively noisy histograms obtained from a single field of view. A post synchronization technique [33] was therefore used in order to combine the results from multiple fields of view to generate better-defined histograms.

Lipid-mixing event detection can be performed with a similar method. However, due to the possibility of multiple step increases in one single time trace, i.e. outer leaflet mixing, followed by inner leaflet mixing, full automation requires both lipid and content dye fluorescence intensity time traces for a particular vesicle-vesicle pair.

Cryo-electron microscopy provides quantitative analysis of vesicle fusion

Electron microscopy (EM) has been used to study synaptic vesicles since the early days of molecular neurobiology. Early work mainly focused on the localizations and morphologies of synaptic vesicles under various conditions [34, 35]. In such cases, samples were directly dissected from tissues followed by fixation, staining, embedment and section. EM has also been used to examine the components of differential centrifugation experiments, which resulted in methods to isolate so-called synaptosomes from brain extracts [36]. Using antibody labeling and electron microscopy, the synaptic protein synaptobrevin (VAMP) was identified and characterized [37]. More recent work used labeling with a photo-convertible fluorescent dye and serial thin sections to generate a three-dimensional reconstruction of the synapse. Combined with quantitative analysis, different populations of synaptic vesicles at hippocampal synapses were identified [38].

Most of the studies mentioned above used negative-staining EM. This method has also been used for studies of vesicle fusion using vesicles derived from in vitro reconstitution. A typical application of negative-staining EM allows one to monitor large morphological changes of vesicles under various conditions [39–42]. However, it is known that negative staining may cause artifacts due to the necessary dehydration step as well as the stain introduced [43, 44]. The resulting deformations of synaptic vesicles are sometimes quite significant [40, 42]. Therefore, negative-staining EM should be used with caution when studying vesicles.

With the advent of cryo-EM, samples can be embedded into vitreous ice without dehydration. Together with the low dose mode of modern electron microscopes, the radiation damage can be significantly limited, leading to atomic resolution in some cases [45]. Cryo-EM has been applied to study SNARE-mediated vesicle fusion [5, 19, 46–48]. Vesicles embedded in vitreous ice were not deformed, allowing low-resolution visualization of membrane morphology and protein density [46, 48]. Furthermore, measurements of vesicle diameters are possible with cryo-EM, and can be used to indicate the occurrence of fusion based on size distributions [5, 47].

Two recent studies used cryo-EM for quantitative analysis of vesicle fusion [8, 49]. The most prominent features of lipid membranes are the electron-dense head groups, rich in phosphorous atoms, which appear as high contrast dark lines when observed on end. A liposome bilayer membrane appears as two parallel black lines at its circumference. When mixed together, reconstituted vesicles with synaptic proteins involved in vesicle fusion formed several types of interfaces based on the number of dark lines and their respective distance at the interface [8] (Fig. 4):

(1) *Point contact*: Close apposition between two vesicles with a distance of 1–5 nm between bilayers, without merging or membrane deformation. The observed interface was typically ≤10 nm along the membrane direction.
(2) *Hemifusion diaphragm*: Extended (>10 nm along membrane) double-layer (two lines) contact between two vesicles, accompanied by flattening at the interface.

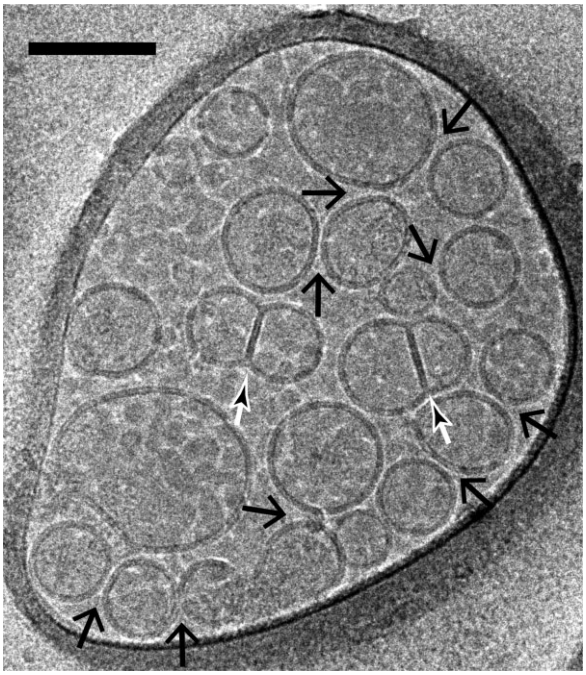

Figure 4. Imaging of vesicle-vesicle morphologies by cryo-electron microscopy. Shown are mixtures of v- (with reconstituted synaptobrevin-2) and t-vesicles (with reconstituted syntaxin-1A and SNAP-25A), which were imaged in the holes of the substrate carbon film, visible as the darker areas in the image, in conditions that clearly show the lipid bilayers. Point contacts (i.e. appositions with small (1–5 nm) separation between vesicles but without merger or deformation of membranes) between docked vesicles were observed (large black arrows) along with hemifused diaphragms (small white/black arrows).The scale bar is 100 nm.

(3) *Extended close contact*: Prolonged contact between bilayers characterized by a triple-line feature over distances $\geq$10 nm along the interface, with a denser (darker) middle line suggesting a close ($<$1 nm) double-bilayer contact, accompanied by membrane flattening near the interface.
(4) *Mixed interface*: Transition from an extended close contact (characterized by three lines) and a hemifusion diaphragm (characterized by two lines) within a single vesicle-vesicle interface.

For the quantitative interface analysis, the interfaces were selected individually using ''boxer'' feature in EMAN [50] and measured for both before and after Ca^{2+} addition, respectively. The images were then related to real-time monitoring of single vesicle-vesicle fusion, providing complementary information to the fluorescence intensity traces. In particular, the relative abundance of each type of interface was determined for the time point that the vesicles were flash-frozen for cryo-EM. This quantitative analysis of vesicle interfaces was performed by visual inspection of many ($\sim$30) EM micrographs, all taken in the same condition, producing statistically significant results.

With cryo-EM micrographs, it is also possible to determine the distance between the membranes measured from two-dimensional density profiles of the EM images. It is expected that the distance is dependent on synaptic proteins, including SNAREs, synaptotagmin and complexin. As a first attempt, models of proteins were fitted into the putative density observed in some of the EM images and provided a first glimpse of the minimal Ca^{2+}-triggered fusion machinery consisting of neuronal SNAREs and synaptotagmin-1 [8].

A follow-up study would systematically evaluate the populations of different interfaces with combinations of various regulatory proteins, reagents, and conditions. Measuring distances between membranes for each type of membrane interface may reveal the intricate regulatory roles of different synaptic proteins. Clearly, the development of automatic image processing will be critical in order to reduce human bias and reduce the time required to analyze the EM micrographs. Another promising direction would be to obtain an image of the fusion machine at the fusion junction by three-dimensional tomography. Although the proteins involved in fusion are generally small and difficult to visualize, high-resolution structural information from crystallography [51, 52] as well as single molecule fluorescence resonance energy transfer experiments (smFRET) [53] could be combined with EM tomograms to obtain a hybrid model of the vesicle fusion machinery before and after fusion. Furthermore, with future advances in technology, we expect that higher resolution images can be obtained by cryo-EM.

Conclusions and outlook: Extension of the Ca^{2+} delivery method for mimicking trains of action potentials

In vitro protein-reconstituted proteoliposome assays are commonly used to study SNARE-mediated membrane fusion. However, many ensemble and single-vesicle experiments have been performed with lipid mixing, but not content mixing, indicators. Through a combination of advanced single-molecule technique and cryo-EM, we found that there is no direct correlation between lipid and content mixing in Ca^{2+}-triggered fast fusion. Lipid mixing events can occur seconds before content mixing, or in many cases, no content mixing [8]. Our results suggest that protein-reconstituted proteoliposome experiments for fast fusion should always employ content-mixing indicators in addition to, or in place of, lipid-mixing indicators.

Fast fusion events and metastable membrane fusion intermediates are expected to occur upon a Ca^{2+} spike during an action potential. Normally, synaptic release sites comprise a readily releasable pool of 200–300 vesicles, with a probability per action potential ranging from 0.05 to 0.9 that a synaptic vesicle will fuse [54, 55]. In addition to up-stream regulation, such as the synaptic vesicle reserve pool, these Ca^{2+}-triggered intermediates might serve as a tuning mechanism to ensure a sufficient number of release events per subsequent action potential. Such a buffering mechanism could mediate synaptic activity before using the reserve pool upon a high level of synaptic stimulation [54, 56]. Moreover, preventing the occurrence of metastable intermediates upon Ca^{2+} influx could be a possible regulatory function of other factors during

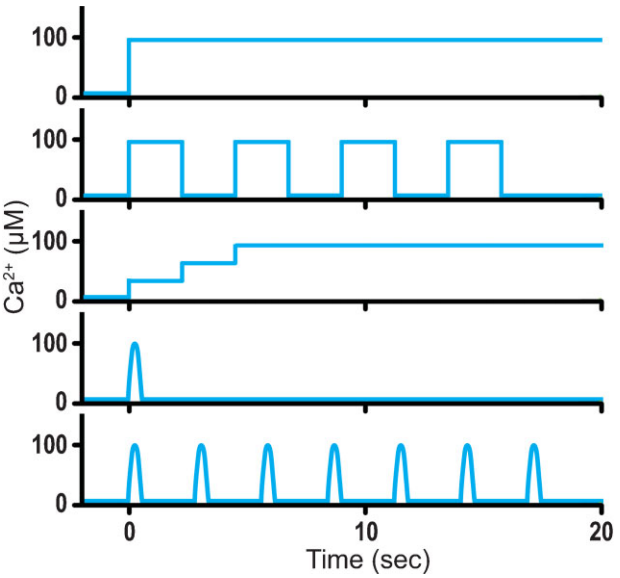

Figure 5. Possible Ca^{2+}-concentration profiles. Shown are a one-step function, a multi-step function, a step function with increasing concentration, a short pulse, and multiple short pulses.

fast Ca^{2+}-triggered membrane fusion. Downstream buffering via metastable fusion intermediates suggests a mechanism for providing a sufficient number of readily releasable synaptic vesicles while preserving the reserve pool.

In order to study the molecular mechanism of a series of fusion events triggered by Ca^{2+} in vitro, besides a one-step Ca^{2+} concentration profile, other Ca^{2+}-concentration profiles, such as a multi-step function and a step function with increasing concentration (Fig. 5), should be developed. Such Ca^{2+}-concentration profiles could be accomplished by using microfluidic techniques. Our single vesicle-vesicle assay could then be used to mimic trains of action potentials in neurons. With such developments, combined with fast imaging techniques to enable measurement of the rise time, similar to those used in recent studies of virus fusion [57, 58], we hope to obtain a ''molecular movie'' of Ca^{2+}-triggered membrane fusion on a millisecond time scale.

Acknowledgments

We thank Steven Chu for a long-term collaboration leading to the single vesicle-vesicle fusion assay, Rex Garland for help with the automation of data analysis and Sachi Shah & Amie Nguyen for help with protein purification. This work was supported by the Fundamental Research Funds for the Central Universities (Xi'an Jiaotong University to J.D.) and the National Institutes of Health (R37-MH63105 to A.T.B.).

References

1. **Sudhof TC**, **Rothman JE.** 2009. Membrane fusion: grappling with SNARE and SM proteins. *Science* **323**: 474–7.
2. **Struck DK**, **Hoekstra D**, **Pagano RE.** 1981. Use of resonance energy transfer to monitor membrane fusion. *Biochemistry* **20**: 4093–9.
3. **Weber T**, **Zemelman BV**, **McNew JA**, **Westermann B**, et al. 1998. SNAREpins: minimal machinery for membrane fusion. *Cell* **92**: 759–72.
4. **Bowen ME**, **Weninger K**, **Brunger AT**, **Chu S.** 2004. Single molecule observation of liposome-bilayer fusion thermally induced by soluble *N*-ethyl maleimide sensitive-factor attachment protein receptors (SNAREs). *Biophys J* **87**: 3569–84.
5. **Kyoung M**, **Srivastava A**, **Zhang YX**, **Diao JJ**, et al. 2011. In vitro system capable of differentiating fast Ca(2 +)-triggered content mixing from lipid exchange for mechanistic studies of neurotransmitter release. *Proc Natl Acad Sci USA* **108**: E304–13.
6. **Floyd DL**, **Ragains JR**, **Skehel JJ**, **Harrison SC**, et al. 2008. Single-particle kinetics of influenza virus membrane fusion. *Proc Natl Acad Sci USA* **105**: 15382–7.
7. **Jun Y**, **Wickner W.** 2007. Assays of vacuole fusion resolve the stages of docking, lipid mixing, and content mixing. *Proc Natl Acad Sci USA* **104**: 13010–5.
8. **Diao J**, **Grob P**, **Cipriano DJ**, **Kyoung M**, et al. 2012. Synaptic proteins promote calcium-triggered fast transition from point contact to full fusion. *eLife* **1**: e00109.
9. **Cypionka A**, **Stein A**, **Hernandez JM**, **Hippchen H**, et al. 2009. Discrimination between docking and fusion of liposomes reconstituted with neuronal SNARE-proteins using FCS. *Proc Natl Acad Sci USA* **106**: 18575–80.
10. **Diao J**, **Ishitsuka Y**, **Bae WR.** 2011. Single-molecule FRET study of SNARE-mediated membrane fusion. *Biosci Rep* **31**: 457–63.
11. **Diao J**, **Su ZL**, **Lu XB**, **Yoon TY**, et al. 2010. Single-vesicle fusion assay reveals Munc 18-1 binding to the SNARE core is sufficient for stimulating membrane fusion. *ACS Chem Neurosci* **1**: 168–74.
12. **Yoon TY**, **Lu X**, **Diao JJ**, **Lee SM**, et al. 2008. Complexin and Ca(2 +) stimulate SNARE-mediated membrane fusion. *Nat Struct Mol Biol* **15**: 707–13.
13. **Kyoung M**, **Zhang Y**, **Diao J**, **Chu S**, et al. 2012. Studying calcium-triggered vesicle fusion in a single vesicle-vesicle content and lipid-mixing system. *Nat Protoc* **8**: 1–16.
14. **Kim JY**, **Choi BK**, **Choi MG**, **Kim SA**, et al. 2012. Solution single-vesicle assay reveals PIP2-mediated sequential actions of synaptotagmin-1 on SNAREs. *EMBO J* **31**: 2144–55.
15. **Chan YHM**, **van Lengerich B**, **Boxer SG.** 2009. Effects of linker sequences on vesicle fusion mediated by lipid-anchored DNA oligonucleotides. *Proc Natl Acad Sci USA* **106**: 979–84.
16. **Sorensen JB.** 2009. Conflicting views on the membrane fusion machinery and the fusion pore. *Annu Rev Cell Dev Bi* **25**: 513–37.
17. **Schneggenburger R**, **Neher E.** 2000. Intracellular calcium dependence of transmitter release rates at a fast central synapse. *Nature* **406**: 889–93.
18. **Wang Z**, **Liu H**, **Gu Y**, **Chapman ER.** 2011. Reconstituted synaptotagmin I mediates vesicle docking, priming, and fusion. *J Cell Biol* **195**: 1159–70.
19. **van den Bogaart G**, **Thutupalli S**, **Risselada JH**, **Meyenberg K**, et al. 2011. Synaptotagmin-1 may be a distance regulator acting upstream of SNARE nucleation. *Nat Struct Mol Biol* **18**: 805–12.
20. **Lee HK**, **Yang Y**, **Su ZL**, **Hyeon C**, et al. 2010. Dynamic Ca(2 +)-dependent stimulation of vesicle fusion by membrane-anchored Synaptotagmin 1. *Science* **328**: 760–3.
21. **Diao J**, **Ishitsuka Y**, **Lee H**, **Joo C**, et al. 2012. A single vesicle-vesicle fusion assay for in vitro studies of SNAREs and accessory proteins. *Nat Protoc* **7**: 921–34.
22. **Diao J**, **Su ZL**, **Ishitsuka Y**, **Lu B**, et al. 2010. A single-vesicle content mixing assay for SNARE-mediated membrane fusion. *Nat Commun* **1**: 54.
23. **Lai Y**, **Diao J**, **Liu Y**, **Ishitsuka Y**, et al. 2013. Fusion pore formation and expansion induced by Ca2+ and synaptotagmin 1. *Proc Natl Acad Sci USA* **110**: 1333–8.
24. **Shi L**, **Shen QT**, **Kiel A**, **Wang J**, et al. 2012. SNARE proteins: one to fuse and three to keep the nascent fusion pore open. *Science* **335**: 1355–9.
25. **Ma C**, **Su L**, **Seven AB**, **Xu Y**, et al. 2013. Reconstitution of the vital functions of Munc18 and Munc13 in neurotransmitter release. *Science* **339**: 421–5.
26. **Zucchi PC**, **Zick M.** 2011. Membrane fusion catalyzed by a Rab, SNAREs, and SNARE chaperones is accompanied by enhanced permeability to small molecules and by lysis. *Mol Biol Cell* **22**: 4635–46.
27. **Joo C**, **Balci H**, **Ishitsuka Y**, **Buranachai C**, et al. 2008. Advances in single-molecule fluorescence methods for molecular biology. *Annu Rev Biochem* **77**: 51–76.
28. **Wang YZ.** 1995. Jump and sharp cusp detection by wavelets. *Biometrika* **82**: 385–97.
29. **Rudin LI**, **Osher S**, **Fatemi E.** 1992. Nonlinear total variation based noise removal algorithms. *Physica D* **60**: 259–68.

30. **Lin DC**, **Dimitriadis EK**, **Horkay F.** 2007. Robust strategies for automated AFM force curve analysis - I. Non-adhesive indentation of soft, inhomogeneous materials. *J Biomech Eng-T ASME* **129**: 430–40.
31. **Wald A**, **Wolfowitz J.** 1940. On a test whether two samples are from the same population. *Ann Math Stat* **11**: 147–62.
32. **Diao J**, **Burre J**, **Vivona S**, **Cipriano DJ**, et al. 2013. Native α-synuclein induces clustering of synaptic vesicle mimics via binding to phospholipids and synaptobrevin-2/VAMP2. *eLife* **2**: e00592.
33. **Marshall RA**, **Aitken CE**, **Dorywalska M**, **Puglisi JD.** 2008. Translation at the single-molecule level. *Annu Rev Biochem* **77**: 177–203.
34. **Gray EG**, **Whittaker VP.** 1962. Isolation of nerve endings from brain – an electron-microscopic study of cell fragments derived by homogenization and centrifugation. *J Anat* **96**: 79–88.
35. **Whittaker VP**, **Gray EG.** 1962. The synapse: biology and morphology. *Brit Med Bull* **18**: 223–8.
36. **Whittaker VP**, **Michaelson IA**, **Kirkland RJ.** 1964. Separation of synaptic vesicles from nerve-ending particles (synaptosomes). *Biochem J* **90**: 293–303.
37. **Baumert M**, **Maycox PR**, **Navone F**, **Decamilli P**, et al. 1989. Synaptobrevin – an integral membrane-protein of 18000 Daltons present in small synaptic vesicles of rat-brain. *EMBO J* **8**: 379–84.
38. **Schikorski T**, **Stevens CF.** 2001. Morphological correlates of functionally defined synaptic vesicle populations. *Nat Neurosci* **4**: 391–5.
39. **Groffen AJ**, **Martens S**, **Arazola RD**, **Cornelisse LN**, et al. 2010. Doc2b is a high-affinity Ca2+ sensor for spontaneous neurotransmitter release. *Science* **327**: 1614–8.
40. **Hui EF**, **Johnson CP**, **Yao J**, **Dunning FM**, et al. 2009. Synaptotagmin-mediated bending of the target membrane is a critical step in Ca(2+)-regulated fusion. *Cell* **138**: 709–21.
41. **Diao J**, **Yoon TY**, **Su ZL**, **Shin YK**, et al. 2009. C2AB: a molecular glue for lipid vesicles with a negatively charged surface. *Langmuir* **25**: 7177–80.
42. **Martens S**, **Kozlov MM**, **McMahon HT.** 2007. How synaptotagmin promotes membrane fusion. *Science* **316**: 1205–8.
43. **Bremer A**, **Henn C**, **Engel A**, **Baumeister W**, et al. 1992. Has negative staining still a place in biomacromolecular electron-microscopy. *Ultramicroscopy* **46**: 85–111.
44. **Hsieh CE**, **Leith A**, **Mannella CA**, **Frank J**, et al. 2006. Towards high-resolution three-dimensional imaging of native mammalian tissue: electron tomography of frozen-hydrated rat liver sections. *J Struct Biol* **153**: 1–13.
45. **Zhou ZH.** 2008. Towards atomic resolution structural determination by single-particle cryo-electron microscopy. *Curr Opin Struc Biol* **18**: 218–28.
46. **Xu Y**, **Seven AB**, **Su L**, **Jiang QX**, et al. 2011. Membrane bridging and hemifusion by denaturated Munc18. *Plos ONE* **6**: e22012.
47. **Holt M**, **Riedel D**, **Stein A**, **Schuette C**, et al. 2008. Synaptic vesicles are constitutively active fusion machines that function independently of Ca(2+). *Curr Biol* **18**: 715–22.
48. **Arac D**, **Chen XC**, **Khant HA**, **Ubach J**, et al. 2006. Close membrane-membrane proximity induced by Ca^{2+}-dependent multivalent binding of synaptotagmin-1 to phospholipids. *Nat Struct Mol Biol* **13**: 209–17.
49. **Hernandez JM**, **Stein A**, **Behrmann E**, **Riedel D**, et al. 2012. Membrane fusion intermediates via directional and full assembly of the SNARE complex. *Science* **336**: 1581–4.
50. **Ludtke SJ**, **Baldwin PR**, **Chiu W.** 1999. EMAN: semiautomated software for high-resolution single-particle reconstructions. *J Struct Biol* **128**: 82–97.
51. **Vrljic M**, **Strop P**, **Ernst JA**, **Sutton RB**, et al. 2010. Molecular mechanism of the synaptotagmin-SNARE interaction in Ca(2+)-triggered vesicle fusion. *Nat Struct Mol Biol* **17**: 325–31.
52. **Sutton RB**, **Fasshauer D**, **Jahn R**, **Brunger AT.** 1998. Crystal structure of a SNARE complex involved in synaptic exocytosis at 2.4 angstrom resolution. *Nature* **395**: 347–53.
53. **Choi UB**, **Strop P**, **Vrljic M**, **Chu S**, et al. 2010. Single-molecule FRET-derived model of the synaptotagmin 1-SNARE fusion complex. *Nat Struct Mol Biol* **17**: 318–24.
54. **Rizzoli SO**, **Betz WJ.** 2005. Synaptic vesicle pools. *Nat Rev Neurosci* **6**: 57–69.
55. **Dobrunz LE**, **Stevens CF.** 1997. Heterogeneity of release probability, facilitation, and depletion at central synapses. *Neuron* **18**: 995–1008.
56. **Denker A**, **Bethani I**, **Krohnert K**, **Korber C**, et al. 2011. A small pool of vesicles maintains synaptic activity in vivo. *Proc Natl Acad Sci USA* **108**: 17177–82.
57. **Ivanovic T**, **Choi J**, **Whelan S**, **van Oijen A**, et al. 2013. Influenza-virus membrane fusion: cooperative fold-back of stochastically induced hemagglutinin intermediates. *eLife* **2**: e00333.
58. **Ivanovic T**, **Rozendaal R**, **Floyd DL**, **Popovic M**, et al. 2012. Kinetics of proton transport into influenza virions by the viral M2 channel. *Plos ONE* **7**: e31566.